

Simulating spin dynamics with spin-dependent cross sections in heavy-ion collisions

Yin Xia,^{1,2} Jun Xu*,¹ Bao-An Li,^{3,4} and Wen-Qing Shen¹

¹*Shanghai Institute of Applied Physics, Chinese Academy of Sciences, Shanghai 201800, China*

²*University of Chinese Academy of Sciences, Beijing 100049, China*

³*Department of Physics and Astronomy, Texas A&M University-Commerce, Commerce, TX 75429-3011, USA*

⁴*Department of Applied Physics, Xi'an Jiao Tong University, Xi'an 710049, China*

(Dated: June 16, 2021)

We have incorporated the spin-dependent nucleon-nucleon cross sections into a Boltzmann-Uehling-Uhlenbeck transport model for the first time, using the spin-singlet and spin-triplet nucleon-nucleon elastic scattering cross sections extracted from the phase-shift analyses of nucleon-nucleon scatterings in free space. We found that the spin splitting of the collective flows is not affected by the spin-dependent cross sections, justifying it as a good probe of the in-medium nuclear spin-orbit interaction. With the in-medium nuclear spin-orbit mean-field potential that leads to local spin polarization, we found that the spin-averaged observables, such as elliptic flows of free nucleons and light clusters, becomes smaller with the spin-dependent differential nucleon-nucleon scattering cross sections.

PACS numbers: 25.70.-z, 13.88.+e, 21.10.Hw, 24.10.Lx, 21.30.Fe

I. INTRODUCTION

The spin-orbit interaction, which was previously introduced to explain the magic number of finite nuclei, is critical in understanding the structures of rare isotopes and their impacts on astrophysics [1–5]. Heavy-ion collisions provide the only way of studying properties of nuclear matter as well as nuclear interactions at both finite densities and temperatures in terrestrial laboratories, and a useful means of extracting properties of the in-medium nuclear spin-orbit interaction with optimal reaction conditions. Recently, we have developed a spin- and isospin-dependent Boltzmann-Uehling-Uhlenbeck (SIBUU) transport model, by incorporating the nucleon spin degree of freedom and the nuclear spin-orbit interaction into the IBUU transport model [6, 7]. We found this model is useful in studying the spin dynamics in intermediate-energy heavy-ion collisions [8]. In particular, it was observed that the spin splittings of collective flows of free nucleons and light clusters can be good probes of the in-medium spin-orbit interaction [9, 10]. However, in our previous studies, we applied the spin-dependent mean-field potential for nucleons but employed the spin-averaged nucleon-nucleon scattering cross sections. In order to have a complete framework of the spin-dependent transport approach and a better description of the spin dynamics in intermediate-energy heavy-ion collisions, in the present study we incorporated the spin-singlet and spin-triplet cross sections for elastic nucleon-nucleon scatterings into the model. The latter are extracted based on the phase-shift analyses of nucleon-nucleon scatterings in free space. We found that the spin splitting of the collective flow as a probe of the in-medium nuclear spin-orbit interaction is almost not af-

ected by the spin-dependent nucleon-nucleon scattering cross sections. However, the overall elliptic flows of free nucleons and light clusters are slightly smaller with the spin-dependent nucleon-nucleon scattering cross sections compared with the spin-averaged ones, if there is local spin polarization induced by the spin-dependent mean-field potential. A more complete BUU framework including both the spin-dependent potential and the spin-dependent cross sections has been established, providing possibilities of further exploring the interesting physics of spin dynamics in intermediate-energy heavy-ion collisions.

II. SPIN-DEPENDENT CROSS SECTIONS FROM PHASE-SHIFT ANALYSES

The phase-shift analysis has been an effective way of decoupling nucleon-nucleon interactions into various channels by fitting experimental nucleon-nucleon scattering data in terms of the scattering matrix [11–14]. There are series of studies on the energy-dependent phase-shift analyses of nucleon-nucleon elastic scattering data in a wide energy range [15–17]. Using the phase-shift data in Ref. [15], we evaluate the spin-singlet and spin-triplet nucleon-nucleon elastic cross sections within the incident nucleon energy range between 1 and 500 MeV, where the inelastic scatterings are less important. For completeness, we first recall the most relevant formulae in the following.

We begin with the general formula for the differential cross section of two-body collisions expressed directly in terms of the eigenphases of the scattering matrix by Blatt and Biedenharn [18]:

$$d\sigma^{\alpha's';\alpha s} = \frac{g}{(2s+1)k^2} \sum_{L=0}^{\infty} B_L(\alpha's';\alpha s) P_L(\cos\theta) d\Omega, \quad (1)$$

*corresponding author: xujun@sinap.ac.cn

where g is 1 for neutron-proton scatterings and 4 for proton-proton (neutron-neutron) scatterings, $P_L(\cos\theta)$ is the Legendre polynomial, k is the center-of-mass (C.M.) momentum in the two-body system, and the coefficients

$$\begin{aligned}
B_L(\alpha' s'; \alpha s) &= \frac{(-)^{s'-s}}{4} \sum_{J_1} \sum_{J_2} \sum_{l_1} \sum_{l_2} \sum_{l_1'} \sum_{l_2'} \\
&\times Z(l_1 J_1 l_2 J_2, s L) Z(l_1' J_1 l_2' J_2, s' L) \\
&\times R.P. [(\delta_{\alpha'\alpha} \delta_{s's} \delta_{l_1' l_1} - S_{\alpha' s' l_1'; \alpha s l_1}^{J_1})^* \\
&\times (\delta_{\alpha'\alpha} \delta_{s's} \delta_{l_2' l_2} - S_{\alpha' s' l_2'; \alpha s l_2}^{J_2})] \quad (2)
\end{aligned}$$

can be determined directly from the phase-shift data. In the above expression, δ_{ab} represents the Kronecker δ function; α , s , l , and J represent the scattering channel, the spin of the scattering channel, the orbital angular momentum, and the total angular momentum, respectively; $S_{\alpha' s' l'; \alpha s l}^J$ is the scattering amplitude of a collision from a channel $\alpha s l$ to a channel $\alpha' s' l'$; the Z coefficient represents the selection rules introduced by Biedenharn *et al.* [19]; the $R.P.[\dots]$ represents the real part of the expression in the bracket. In the limit of pure elastic nucleon-nucleon scatterings without spin flipping, $\alpha' = \alpha$ and $s' = s$ are always satisfied, so we omit the superscript α and use only s as the superscript in the following. $s = 0$ and $s = 1$ stand for the spin-singlet and spin-triplet scattering, respectively.

Let's first consider the spin-singlet and spin-triplet channel for neutron-proton scatterings. For the spin-singlet case with $s = 0$, there is only one channel $l = J$. Using $S = \exp(2i\delta_J^0)$, Eq. (2) becomes

$$\begin{aligned}
B_L(0; 0) &= \sum_{J_1} \sum_{J_2} \sum_{l_1=J_1} \sum_{l_2=J_2} Z(l_1 J_1 l_2 J_2, 0 L)^2 \\
&\times \sin \delta_{J_1}^0 \sin \delta_{J_2}^0 \cos(\delta_{J_1}^0 - \delta_{J_2}^0), \quad (3)
\end{aligned}$$

where δ_J^0 is the phase-shift of the spin-singlet channel with orbital angular momentum $l = J$. For the spin-triplet case with $s = 1$, given $l = J$, there is still only one channel with $S = \exp(2i\delta_J^1)$. When the neutron-proton scattering is affected by the tensor force in their spin-triplet state, the angular momentum l can have two values, i.e., $l = J \pm 1$. In the latter case, the general expression of the S matrix of a two-channel reaction is

$$\begin{aligned}
S &= \\
&\begin{pmatrix} \cos^2(\epsilon_J) e^{2i\delta_J^1-1} + \sin^2(\epsilon_J) e^{2i\delta_J^1+1} & \frac{1}{2} \sin(2\epsilon_J) (e^{2i\delta_J^1-1} - e^{2i\delta_J^1+1}) \\ \frac{1}{2} \sin(2\epsilon_J) (e^{2i\delta_J^1-1} - e^{2i\delta_J^1+1}) & \sin^2(\epsilon_J) e^{2i\delta_J^1-1} + \cos^2(\epsilon_J) e^{2i\delta_J^1+1} \end{pmatrix} \quad (4)
\end{aligned}$$

In the above, $\delta_{J\pm 1}^1$ is usually called the Biedenharn-Blatt (BB) phase shift of the spin-triplet channel with $l = J \pm 1$, and ϵ_J is the parameter describing the mixing probability of the two coupling states. By using the energy-dependent neutron-proton phase-shift data as well as the mixing parameters for various channels in Tables III and IV of Ref. [15], we calculate the coefficient B_L and the

differential cross section. For the unpolarized neutron-proton cross section, we also take the summation of the isovector contribution $T = 1$, the isoscalar contribution $T = 0$, and their interference contribution to the coefficient B_L [20]. We note there is a simplified method for calculating the spin-triplet case developed by Blatt and Biedenharn [21], and it leads to identical results.

For proton-proton scatterings, we only incorporate the nuclear contribution to the cross section into transport model simulations, but subtract the contribution of the long-range Coulomb potential to the scatterings. For the spin-singlet and spin-triplet proton-proton scatterings with $l = J$, the scattering matrix S can be expressed as

$$S = e^{2i\delta_J^{0(1)}} - e^{2i\phi_J} + 1, \quad (5)$$

where ϕ_J is the pure Coulomb phase shift for orbital angular momentum $l = J$, and it can be written as [22]

$$\phi_l = \sum_{m=1}^l \arctan(\eta/m), \quad (6)$$

with $\eta = e^2/\hbar v \approx (137\beta)^{-1}$ where $\beta = v/c$ is the reduced velocity of the incident proton in the lab frame. In order to subtract the Coulomb contribution from the S matrix for the two channels of spin-triplet scatterings with $l = J \pm 1$, we express it as [23]

$$\begin{aligned}
S &= 1 + \\
&\begin{pmatrix} \cos(2\epsilon_J) e^{2i\delta_{J-1}^1} - e^{2i\phi_{J-1}} & i \sin(2\epsilon_J) e^{i(\delta_{J+1}^1 + \delta_{J-1}^1)} \\ i \sin(2\epsilon_J) e^{i(\delta_{J+1}^1 + \delta_{J-1}^1)} & \cos(2\epsilon_J) e^{2i\delta_{J+1}^1} - e^{2i\phi_{J+1}} \end{pmatrix}, \quad (7)
\end{aligned}$$

with

$$\delta_l^{0(1)} = \delta_l^{0(1)}(N) + \phi_l \quad (8)$$

where $\delta_l^{0(1)}(N)$ is called the nuclear bar phase shifts, which are taken from Table II of Ref. [15] for various proton incident energies. The way of subtracting the Coulomb contribution assumes that the Coulomb force acts only outside the region of the nuclear force where the WKB approximation is valid [23]. For the spin-singlet and spin-triplet proton-proton scatterings with $l = J$, the expressions for the scattering matrix S are the same for BB phase shifts and bar phase shifts, as can be seen from Eq. (5). In this way the spin-dependent differential proton-proton elastic scattering cross sections can also be obtained.

III. PARAMETRIZATION OF THE SPIN-DEPENDENT CROSS SECTIONS

Starting from the energy-dependent phase-shift results of nucleon-nucleon scatterings by Arndt *et al.* [15], and using the method described above, we are now able to

obtain the differential cross sections for elastic nucleon-nucleon scatterings at various collision energies. Since the higher-order terms of the Legendre polynomials vanish after intergration, the total cross section is determined by the terms with $L = 0$ in Eq. (1). The total cross sections for both spin-singlet and spin-triplet elastic neutron-proton scatterings between 1 and 500 MeV can be parameterized respectively as

$$\begin{aligned}\sigma_{np}^0 &= 9302.64/E^3 - 982.187/E^2 - 1.32 \times 10^2 + 1.03E \\ &\quad - 3.06 \times 10^{-3}E^2 + 4.85 \times 10^{-6}E^3 - 3.19 \times 10^{-9}E^4, \quad (9) \\ \sigma_{np}^1 &= -27888.84 \times 10^4/E^3 + 17565.39/E^2 + 13382.81/E \\ &\quad - 8.10 \times 10^1 + 0.37E - 2.75 \times 10^{-4}E^2 - 9.60 \times 10^{-7}E^3 \\ &\quad + 1.37 \times 10^{-9}E^4. \quad (10)\end{aligned}$$

Similarly, the total cross sections for both spin-singlet and spin-triplet elastic proton-proton scatterings between 1 and 500 MeV can also be parameterized respectively as

$$\begin{aligned}\sigma_{pp}^0 &= -11877.31/E^3 + 733.31/E^2 + 17397.66/E - 2.38 \times 10^2 \\ &\quad + 1.51E - 4.9 \times 10^{-3}E^2 + 8.37 \times 10^{-6}E^3 - 5.58 \times 10^{-9}E^4, \\ \sigma_{pp}^1 &= -1.20 + 0.79E - 8.40 \times 10^{-3}E^2 + 3.24 \times 10^{-5}E^3, \\ &\quad (1 \text{ MeV} < E < 100 \text{ MeV}) \\ \sigma_{pp}^1 &= 1.72 \times 10^1 + 0.16E - 8.13 \times 10^{-4}E^2 + 2.14 \times 10^{-6}E^3 \\ &\quad - 2.86 \times 10^{-9}E^4 + 1.52 \times 10^{-12}E^5. \\ &\quad (100 \text{ MeV} < E < 500 \text{ MeV})\end{aligned} \quad (11)$$

In the above, σ^0 and σ^1 in mb are the cross sections for the elastic spin-singlet and spin-triplet scatterings, respectively, and E in MeV is the kinetic energy of the incident nucleon in the lab frame. The spin-averaged cross section can be obtained from $\sigma = \sigma^0/4 + 3\sigma^1/4$. In Fig. 1 we compared the total elastic scattering cross sections obtained in the present study with those previously used in the IBUU transport model, with the latter taken from Ref. [24] parameterized as

$$\sigma_{pp(nn)} = 8.76/\beta^2 - 15.04/\beta + 13.73 + 68.76\beta^4, \quad (12)$$

$$\sigma_{np} = 25.26/\beta^2 - 18.18/\beta - 70.67 + 113.85\beta, \quad (13)$$

where the cross section σ is in mb, and $\beta = \sqrt{1 - M_N^2 c^4 / (M_N c^2 + E)^2}$ is the reduced velocity of the incident nucleon with M_N being the nucleon mass. We find that the previously used parameterized cross sections are similar to the spin-averaged ones obtained in the present study using the phase-shift results in the energy range considered. Note that a cut at very low energy region, where the cross section may diverge, is usually used in transport model simulations.

We have also parameterized the differential spin-singlet and spin-triplet cross sections for elastic neutron-proton and proton-proton scatterings between 1 and 500 MeV

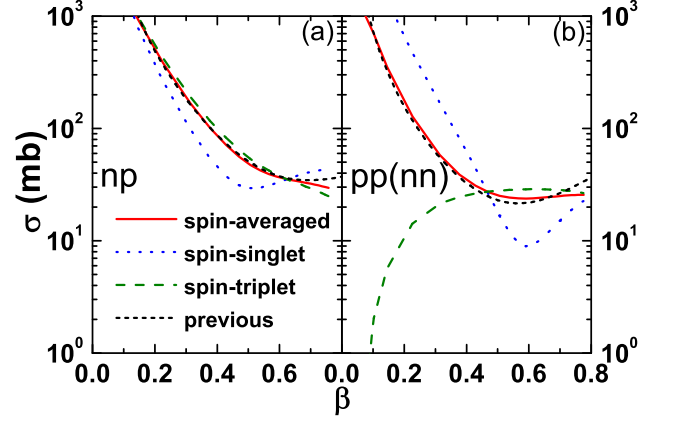


FIG. 1: (color online) Total elastic spin-averaged, spin-singlet, and spin-triplet cross sections obtained in the present study for neutron-proton (left) and proton-proton (neutron-neutron) (right) scatterings as functions of the reduced incident nucleon velocity β in the lab frame, compared with the previous ones used in the IBUU transport model.

in the following form:

$$d\sigma_{np}^s(\theta) = \sum_{n=0}^{11} a_n^s \cos^n \theta d\Omega, \quad (14)$$

$$d\sigma_{pp}^s(\theta) = \sum_{m=0}^5 b_{2m}^s \cos^{2m} \theta d\Omega. \quad (15)$$

In the above equations, the cross sections are in mb, n and m are related to the angular momentum quantum numbers of the orbital wave function, i.e., from s -wave to h -wave, as used in the energy-dependent phase-shift analyses. With the differential cross sections from phase-shift results at discrete energies, we are able to parameterize the coefficients a_n^s and b_{2m}^s as functions of the energy E to get continuous energy-dependent differential cross sections between 1 and 500 MeV. The s -wave coefficients a_0^0 , a_0^1 , b_0^0 , and b_0^1 , which lead to the total cross section, are parameterized respectively as

$$\begin{aligned}a_0^0 &= -47.99/E^3 - 28.93/E^2 + 740.42/E - 12.11 + 7.53 \times 10^{-2}E \\ &\quad - 2.32 \times 10^{-4}E^2 + 3.83 \times 10^{-7}E^3 - 2.62 \times 10^{-10}E^4, \quad (16)\end{aligned}$$

$$\begin{aligned}a_0^1 &= -2435.74/E^3 + 1565.07/E^2 + 1115.4/E - 9.27 + 0.02E \\ &\quad + 1.43 \times 10^{-4}E^2 - 6.04 \times 10^{-7}E^3 + 6.08 \times 10^{-10}E^4, \quad (17)\end{aligned}$$

$$\begin{aligned}b_0^0 &= -987.99/E^3 + 80.497/E^2 + 1409.47/E - 23.51 + 0.148E \\ &\quad - 4.488 \times 10^{-4}E^2 + 7.203 \times 10^{-7}E^3 - 4.72 \times 10^{-10}E^4, \quad (18)\end{aligned}$$

$$\begin{aligned}b_0^1 &= -0.142 + 0.079E - 8.78 \times 10^{-4}E^2 + 3.36 \times 10^{-6}E^3, \\ &\quad (1 \text{ MeV} < E < 100 \text{ MeV})\end{aligned}$$

$$\begin{aligned}b_0^1 &= 1.89 + 9.85 \times 10^3 E - 6.90 \times 10^{-5}E^2 + 1.84 \times 10^{-7}E^3 \\ &\quad - 2.33 \times 10^{-10}E^4 + 1.16 \times 10^{-13}E^5. \quad (19)\end{aligned}$$

$$(100 \text{ MeV} < E < 500 \text{ MeV})$$

For other coefficients a_n^s and b_{2m}^s corresponding to larger orbital angular momentum quantum numbers, polyno-

mial functions are used to fit their energy dependence, and the fitting results are showed in Table I.

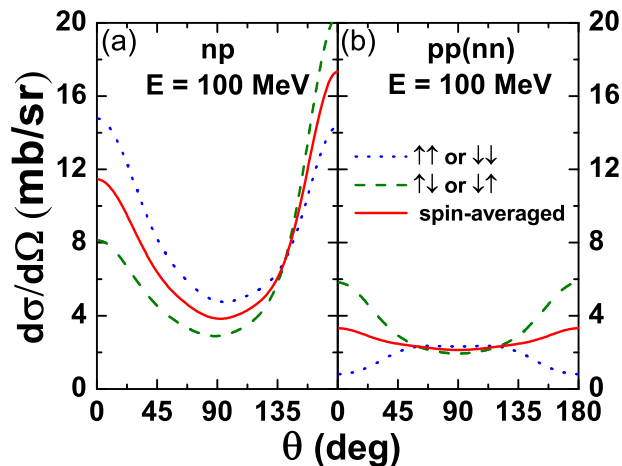


FIG. 2: (color online) Differential cross sections for neutron-proton (left) and proton-proton (right) pairs with the same spin, different spins, and the spin-averaged differential cross sections as functions of the scattering polar angle θ in the C.M. frame, at an incident nucleon energy of 100 MeV.

In transport model simulations of heavy-ion collisions, it is more convenient to use the cross sections determined by the spins of the colliding nucleons, and they can be expressed in terms of the spin-singlet and spin-triplet scattering cross section as

$$\sigma_{NN}^{\uparrow\uparrow(\downarrow\downarrow)} = \sigma_{NN}^1, \quad (20)$$

$$\sigma_{NN}^{\uparrow\downarrow(\downarrow\uparrow)} = (\sigma_{NN}^1 + \sigma_{NN}^0)/2, \quad (21)$$

where $\sigma_{NN}^{\uparrow\uparrow(\downarrow\downarrow)}$ ($\sigma_{NN}^{\uparrow\downarrow(\downarrow\uparrow)}$) is the cross section for nucleon pairs with the same (different) spin with respect to the angular momentum of the pair. The angular dependence of the differential cross sections to be used in SIBUU transport model simulations is plotted in Fig. 2. These angular distributions reveal the nucleon interaction in vacuum. For example, in neutron-proton scatterings, the forward peak is due to the Wigner force while the backward peak is due to the Majorana force [25]. On the other hand, scatterings between identical particles with the same spin and isospin are not likely to have forward and backward peaks due to the strong Pauli repulsive effect.

IV. EFFECTS IN HEAVY-ION SIMULATIONS

In the SIBUU transport model, the density of the initial two nuclei is sampled according to the prediction of Skyrme-Hartree-Fock calculations, while the momentum of each nucleon is sampled according to its local density and further boosted by the beam energy. The spin

expectation value of each nucleon is chosen as a unit vector in the 4π solid angle, and it is randomly sampled in the initial stage. As the system begins to evolve, the coordinate \vec{r} , momentum \vec{p} , and spin \vec{s} of each nucleon follow the equations of motion consistently derived from the spin-dependent Boltzmann-Vlasov equation [7] as follows:

$$d\vec{r}/dt = \vec{p}/\sqrt{p^2c^2 + M_N^2c^4} + \nabla_p U^s, \quad (22)$$

$$d\vec{p}/dt = -\nabla U - \nabla U^s, \quad (23)$$

$$d\vec{s}/dt = -\frac{i}{\hbar}[\vec{s}, U^s], \quad (24)$$

where U is the momentum- and spin-independent mean-field potential, and the right-hand side of the third equation denotes the commutator of each component of spin with the spin-dependent mean-field potential U^s . Particularly, the strength, the isospin dependence, and the density dependence of U^s are still under debate and are hot topics in nuclear structure studies [8]. In our previous studies, we have shown that nucleons with different spins may have different dynamics with U^s , and this leads to local spin polarization (see Fig. 1 of Ref. [6] and Fig. 1 of Ref. [10]) as well as the spin splitting of collective flows of free nucleons and light clusters [6, 9, 10]. Here we investigate the effects of nucleon-nucleon scatterings with spin-dependent differential elastic cross sections in heavy-ion collisions. Since the spin expectation direction is known for each nucleon, the spin state of a single nucleon and that of the colliding nucleon pair can be obtained by projecting the spin expectation direction onto the total angular momentum of the incoming nucleon pair. The differential scattering cross sections are then determined from the spin state as well as the collision energy through the parameterizations given in Sec. III, and they are technically incorporated according to the scattering treatment in Appendix B of Ref. [26].

We first examine the effects of the spin-dependent cross sections on the spin up-down differential transverse flow defined as [6, 9]

$$F_{ud}(y_r) = \frac{1}{N(y_r)} \sum_{i=1}^{N(y_r)} s_i(p_x)_i, \quad (25)$$

where $N(y_r)$ is the number of nucleons with rapidity y_r , $(p_x)_i$ is the momentum of the i th nucleon in x direction, and s_i is 1(-1) for spin-up (spin-down) nucleons with respect to the total angular momentum of the heavy-ion collision system. As discussed in Refs. [6, 9], the spin-dependent potential U^s gives an additional attractive (repulsive) potential to spin-up (spin-down) nucleons, resulting in their different transverse flows. As shown in the left panel of Fig. 3, F_{ud} vanishes without U^s , with the latter the source of different potentials for spin-up and spin-down nucleons and thus their different transverse flows. With U^s , F_{ud} remain almost the same using the spin-averaged and spin-dependent nucleon-nucleon cross sections, as shown in the right panel of Fig. 3. We have

TABLE I: Coefficients for the polynomial fit of the energy dependence of a_n^s ($n > 0$) and b_{2m}^s ($m > 0$), i.e., $a_n^s(b_{2m}^s) = C_0 + C_1E + C_2E^2 + C_3E^3$ ($1 \text{ MeV} < E < 50 \text{ MeV}$) and $a_n^s(b_{2m}^s) = C_4 + C_5E + C_6E^2 + C_7E^3 + C_8E^4 + C_9E^5$ ($50 \text{ MeV} < E < 500 \text{ MeV}$).

| | C_0 | C_1 | $C_2(10^{-3})$ | $C_3(10^{-5})$ | C_4 | C_5 | $C_6(10^{-3})$ | $C_7(10^{-6})$ | $C_8(10^{-9})$ | $C_9(10^{-12})$ |
|------------|------------------------|------------------------|----------------|----------------|--------|------------------------|----------------|----------------|----------------|-----------------|
| a_1^0 | -6.23 | -0.46 | 32.24 | -42.98 | -2.20 | -2.84×10^{-3} | 0.14 | -0.26 | -0.064 | 0.29 |
| a_2^0 | -0.48 | 0.54 | -21.99 | 24.79 | 4.71 | -7.55×10^{-2} | 0.74 | -2.41 | 3.54 | -1.98 |
| a_3^0 | 0.47 | -0.32 | 7.92 | -4.77 | -8.82 | 0.23 | -1.98 | 6.80 | -10.61 | 6.39 |
| a_4^0 | -4.07×10^{-2} | 11.08 | 5.23 | -9.12 | 0.23 | 0.12 | -1.96 | 7.48 | -12.09 | 7.36 |
| a_5^0 | -0.13 | 9.77×10^{-2} | -11.76 | 15.66 | -1.80 | -0.12 | 1.37 | -5.28 | 8.92 | -5.75 |
| a_6^0 | 4.80×10^{-2} | -3.77×10^{-2} | 4.57 | -5.47 | 3.41 | -0.14 | 3.03 | -12.81 | 21.96 | -13.90 |
| a_7^0 | -2.63×10^{-2} | 1.90×10^{-2} | -1.99 | 2.07 | 1.43 | -0.11 | 1.13 | -4.02 | 6.57 | -4.01 |
| a_8^0 | 2.12×10^{-2} | -1.55×10^{-2} | 1.68 | -2.23 | 0.10 | 0.12 | -2.67 | 11.89 | -21.24 | 13.77 |
| a_9^0 | -2.52×10^{-3} | 1.49×10^{-3} | -0.052 | -0.90 | 2.43 | -6.06×10^{-2} | -0.30 | 1.97 | -3.80 | 2.55 |
| a_{10}^0 | -4.21×10^{-5} | 4.64×10^{-4} | -0.19 | 1.45 | -4.37 | 9.84×10^{-2} | 0.43 | -3.68 | 7.86 | -5.56 |
| a_1^1 | 0.36 | -8.13×10^{-2} | 7.28 | -10.15 | 2.72 | -1.39×10^{-2} | -0.11 | 0.92 | -2.11 | 1.59 |
| a_2^1 | -0.18 | -0.22 | 16.87 | -21.24 | 1.10 | 1.07×10^{-1} | -1.00 | 4.27 | -8.11 | 5.63 |
| a_3^1 | 1.17×10^{-2} | 1.15×10^{-2} | -1.34 | 2.27 | -1.69 | 5.93×10^{-2} | -0.57 | 2.10 | -3.42 | 2.09 |
| a_4^1 | 5.37×10^{-2} | -3.46×10^{-2} | 3.80 | -6.46 | 4.16 | -6.24×10^{-2} | -0.65 | 4.21 | -8.40 | 5.75 |
| a_5^1 | -1.81×10^{-3} | 3.65×10^{-3} | -1.07 | 1.97 | -2.72 | 6.95×10^{-2} | -0.36 | 0.39 | 0.41 | -0.72 |
| a_6^1 | 2.03×10^{-2} | -1.74×10^{-2} | 2.24 | -0.78 | -5.71 | 0.25 | -1.42 | 3.63 | -4.75 | 2.52 |
| a_7^1 | -1.05×10^{-2} | 8.01×10^{-3} | -0.91 | 1.06 | 1.76 | -0.11 | 1.41 | -5.04 | 7.87 | -4.64 |
| a_8^1 | 1.32×10^{-3} | -9.45×10^{-4} | 0.09 | 0.08 | -0.70 | 2.77×10^{-2} | -0.19 | 0.53 | -0.66 | 0.29 |
| a_9^1 | -3.39×10^{-4} | 5.50×10^{-5} | 0.05 | -0.61 | 0.94 | -1.36×10^{-2} | -0.43 | 2.03 | -3.58 | 2.27 |
| a_{10}^1 | -5.08×10^{-5} | 6.50×10^{-5} | -0.01 | 0.09 | -0.08 | -1.16×10^{-3} | 0.11 | -0.48 | 0.81 | -0.48 |
| b_2^0 | -1.24 | -9.83×10^{-1} | -36.74 | 38.86 | 8.51 | -9.91×10^{-2} | 0.47 | -1.27 | 1.84 | -1.04 |
| b_4^0 | 0.16 | -0.12 | 14.36 | -20.55 | 4.01 | 4.33×10^{-2} | -0.87 | 3.07 | -4.73 | 2.91 |
| b_6^0 | 1.44×10^{-2} | -1.02×10^{-2} | 0.99 | -0.35 | -1.62 | 0.064 | 0.0061 | -0.27 | 0.57 | -0.61 |
| b_8^0 | 1.38×10^{-4} | -8.66×10^{-5} | 0.0048 | 0.034 | -0.078 | 0.0022 | 0.0097 | -0.042 | 0.068 | -0.041 |
| b_2^1 | 0.039 | -0.019 | -0.82 | 2.06 | -1.44 | 0.03 | -0.15 | 0.52 | -0.98 | 0.67 |
| b_4^1 | -0.027 | 0.023 | -1.79 | 1.63 | -0.488 | 0.397 | -1.61 | 3.08 | -2.10 | 5.63 |
| b_6^1 | 6.53×10^{-5} | -3.52×10^{-3} | 0.52 | -0.84 | 2.13 | -5.18×10^{-2} | 0.34 | -0.84 | 0.65 | -0.073 |
| b_8^1 | 1.73×10^{-3} | -1.95×10^{-3} | 0.204 | -0.18 | -0.63 | 4.94×10^{-2} | -0.68 | 2.55 | -3.93 | 2.25 |
| b_{10}^1 | -2.30×10^{-3} | 6.16×10^{-3} | -0.021 | 0.15 | -0.29 | -3.78×10^{-3} | 0.23 | -1.04 | 1.75 | -1.07 |

also found that the spin up-down differential transverse flow remains the same for neutrons and protons as well as for energetic nucleons, justifying the validity of F_{ud} as a good probe of the strength, the isospin dependence, and the density dependence of the in-medium nuclear spin-orbit potential [6, 9, 10].

Figure 4 compares the resulting spin-averaged elliptic flows ($v_2 = \langle (p_x^2 - p_y^2)/(p_x^2 + p_y^2) \rangle$) of free nucleons and deuterons from the spin-averaged and spin-dependent nucleon-nucleon scattering cross sections with and without the spin-dependent mean-field potential. It is seen that v_2 of free nucleons is the same from the spin-averaged and spin-dependent cross sections without U^s , while the difference is observed with U^s . The latter is due to the local spin polarization induced by U^s . As is known, v_2 is sensitive to the shear viscosity of the system [27, 28], with the later related to the transport cross section defined as

$$\sigma_{tr} = \int \frac{d\sigma}{d\Omega} (1 - \cos^2 \theta). \quad (26)$$

For a given total σ , a more forward- and backward-peaked differential cross section generally leads to a

smaller transport cross section and a larger shear viscosity. Since locally there can be different numbers of spin-up and spin-down nucleons induced by the spin-dependent mean-field potential, the transport cross section can be different from the spin-averaged and spin-dependent cross sections. This is the reason why the slightly different v_2 is observed in Panel (c) of Fig. 4. We have also studied the formation of light clusters formed in transport simulations, through a dynamical coalescence algorithm from nucleons that are close in coordinate and momentum space [10, 29]. The spin-dependent differential cross sections lead to correlations between the scattering angles of final-state nucleons, resulting in the different final distribution of these light clusters. It is seen from Fig. 4 that slight v_2 difference is observed at midrapidities between results from the spin-averaged cross sections and the spin-dependent ones, and the effect is further enhanced with the spin-dependent mean-field potential.

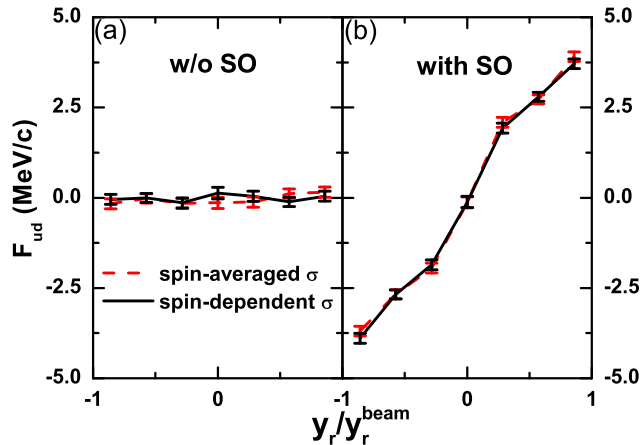


FIG. 3: (color online) Rapidity dependence of the spin differential transverse flow from the spin-averaged and the spin-dependent cross sections with (right) and without (left) the spin-orbit (SO) potential in Au+Au collisions at 100 MeV/nucleon and an impact parameter $b = 12$ fm.

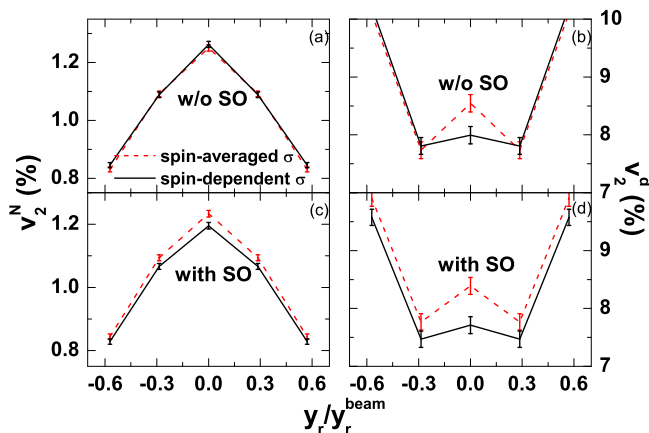


FIG. 4: (color online) Rapidity dependence of the elliptic flow of free nucleons (left) and deuterons (right) from the spin-averaged and the spin-dependent cross sections with (lower) and without (upper) the spin-orbit (SO) potential in Au+Au collisions at 100 MeV/nucleon and an impact parameter $b = 12$ fm.

V. CONCLUSION AND OUTLOOK

Using the phase-shift results from nucleon-nucleon scattering data in free space, we have obtained the spin-

dependent neutron-proton and proton-proton differential elastic scattering cross sections. We have further incorporated them into the spin-dependent Boltzmann-Uehling-Uhlenbeck transport model for the first time. The spin splittings of collective flows, which were previously found as probes of the in-medium nuclear spin-orbit interaction, are not affected by these spin-dependent cross sections. However, spin-averaged quantities, such as the elliptic flows of free nucleons and deuterons, can be slightly affected with both the spin-dependent mean-field potential and cross sections.

We note that it is still a big challenge to obtain the spin-dependent inelastic nucleon-nucleon scattering cross sections in the suitable energy range for intermediate-energy heavy-ion collisions, due to the lack of the experimental data. On the other hand, the in-medium nucleon-nucleon scattering cross sections remain uncertain, even for the spin-independent part. So far, the information of the in-medium cross sections relies on various many-body theories [30–32], while in transport model simulations the in-medium effective mass scaling [33, 34] or empirical parameterizations [35] are generally used. We are still on the way of looking for reliable probes of the in-medium nuclear spin-orbit interaction and studying interesting and relevant physics of spin dynamics in heavy-ion collisions, by using a dynamical framework as complete as possible.

Acknowledgments

We thank Xiao-Ming Xu for helpful communications, and Chen Zhong for maintaining the high-quality performance of the computer facility. This work was supported by the Major State Basic Research Development Program (973 Program) of China under Contract Nos. 2015CB856904 and 2014CB845401, the National Natural Science Foundation of China under Grant Nos. 11320101004, 11475243, and 11421505, the "100-talent plan" of Shanghai Institute of Applied Physics under Grant Nos. Y290061011 and Y526011011 from the Chinese Academy of Sciences, the Shanghai Key Laboratory of Particle Physics and Cosmology under Grant No. 15DZ2272100, the U.S. Department of Energy, Office of Science, under Award Number de-sc0013702, and the CUSTIPEN (China-U.S. Theory Institute for Physics with Exotic Nuclei) under the US Department of Energy Grant No. DEFG02-13ER42025.

-
- [1] P. G. Reinhard and H. Flocard, Nucl. Phys. A **584**, 467 (1995).
 [2] R. J. Furnstahl, John J. Rusnak, and Brian D. Serot, Nucl. Phys. A **632**, 607 (1998).

- [3] M. Bender *et al.*, Phys. Rev. C **60**, 034304 (1999).
 [4] J. P. Schiffer *et al.*, Phys. Rev. Lett. **110**, 169901 (2013).
 [5] L. Gaudefroy *et al.*, Phys. Rev. Lett. **97**, 092501 (2006).
 [6] J. Xu and B. A. Li, Phys. Lett. B **724**, 346 (2013).

- [7] Y. Xia, J. Xu, B. A. Li, and W. Q. Shen, Phys. Lett. B **759**, 596 (2016).
- [8] J. Xu, B. A. Li, W. Q. Shen, and Y. Xia, Front. Phys. **10**, 102501 (2015).
- [9] Y. Xia, J. Xu, B. A. Li, and W. Q. Shen, Phys. Rev. C **89**, 064606 (2014).
- [10] Y. Xia, J. Xu, B. A. Li, and W. Q. Shen, Nucl. Phys. A **955**, 41 (2016).
- [11] E. P. Wigner and L. Eisenbud, Phys. Rev. **72**, 29 (1947).
- [12] L. Wolfenstein, Phys. Rev. **82**, 690 (1951).
- [13] W. Hauser and H. Feshbach, Phys. Rev. **87**, 366 (1952).
- [14] M. H. Macgregor, Phys. Rev. **113**, 1559 (1959).
- [15] R. A. Arndt *et al.*, Phys. Rev. C **15**, 1002 (1977).
- [16] R. A. Arndt *et al.*, Phys. Rev. D **28**, 97 (1983).
- [17] R. A. Arndt *et al.*, Phys. Rev. D **35**, 128 (1987).
- [18] J. M. Blatt and L. C. Biedenharn, Rev. Mod. Phys. **24**, 258 (1952).
- [19] L. C. Biedenharn, J. M. Blatt, and M. E. Rose, Rev. Mod. Phys. **24**, 249 (1952).
- [20] Y. Xia, Ph.D thesis, Shanghai Institute of Applied Physics, 2017.
- [21] J. M. Blatt and L. C. Biedenharn, Phys. Rev. **86**, 399 (1952).
- [22] N. F. Mott and H. S. W. Massey, *Theory of Atomic Collisions* (Clarendon Press, Oxford, 1949), second edition, p. 101.
- [23] H. P. Stapp, T. J. Ypsilantis, and N. Metropolis, Phys. Rev. **105**, 302 (1957).
- [24] S. K. Charagi and S. K. Gupta, Phys. Rev. C **41**, 1610 (1990).
- [25] J. M. Blatt and V. F. Weisskopf, *Theoretical Nuclear Physics* (Springer-Verlag, New York Inc., 1979), p. 178.
- [26] G. F. Bertsch and S. Das Gupta, Phys. Rep. **160**, 189 (1988).
- [27] H. C. Song, S. A. Bass, U. Heinz, T. Hirano, and C. Shen, Phys. Rev. Lett. **106**, 192301 (2011).
- [28] C. L. Zhou, Y. G. Ma, D. Q. Fang, G. Q. Zhang, J. Xu, X. G. Cao, and W. Q. Shen, Phys. Rev. C **90**, 057601 (2014).
- [29] L. W. Chen, C. M. Ko, and B. A. Li, Nucl. Phys. A **729**, 809 (2003).
- [30] G. Q. Li and R. Machleidt, Phys. Rev. C **49**, 566 (1994).
- [31] Q. F. Li, Z. X. Li, and G. J. Mao, Phys. Rev. C **62**, 014606 (2000).
- [32] H. F. Zhang, Z. H. Li, U. Lombardo, P. Y. Luo, F. Sammarruca, and W. Zuo, Phys. Rev. C **76**, 054001 (2007).
- [33] V. R. Pandharipande and S. C. Pieper, Phys. Rev. C **45**, 791 (1991).
- [34] B. A. Li and L. W. Chen, Phys. Rev. C **72**, 064611 (2005).
- [35] D. Klakow, G. Welke, and W. Bauer, Phys. Rev. C **48**, 1982 (1993).